

Ordered Crystalline Film Growth of TIPS-Pentacene and Perovskite by Ultra-sonic Printing and their Application in Photodetectors

Chenning Liu¹, Hang Zhou² and Chuan Liu¹

¹ State Key Laboratory of Optoelectronic Materials and Technologies and the Guangdong Province Key Laboratory of Display Material and Technology, Sun Yat-Sen University, Guangzhou, China

Phone: +86 18102706826 E-mail: liuchuan5@mail.sysu.edu.cn

² Shenzhen Key Lab of Thin Film Transistor and Advanced Display, Peking University Shenzhen Graduate School, Shenzhen, China

Abstract

Organic semiconductors have received great attentions from researchers in the field of flexible electronic because of their higher solubility in organic solvents. Besides the traditional spin coating, there are more and more original technology of printing electronic that have been developed in the solution-processed fabrication.

In this report, we demonstrate and investigate the use of an ultra-sonicated dispenser to guide the formation of crystals of organic and perovskite semiconductors. Highly ordered, aligned crystals are achieved for both organic TIPS-pentacene and perovskite MAPbI₃ semiconductors. The aligned crystals lead to remarkably enhanced electrical performances in an organic thin-film transistor (OTFT) and perovskite photodetector. As a demonstration, we combine the OTFT with photodetectors to achieve an active-matrix of normally off, gate-tunable photodetectors that operate under ambient conditions.

1. Introduction

Inkjet printing electronic technologies have attracted tremendous attentions for the potential use in flexible manufacturing with the competitive advantages of large area, low cost and the capability to print various patterns for matrix or circuits, avoiding the traditional photolithography procedure and potential destruction to the films. However, disconnected drops of ink ejected from the nozzle under pressure could cause discontinuity of the film.

In this research, we utilize an ultra-sonicated dispenser to guide the formation of crystals. The setup and working principle of an ultra-sonicated dispenser is shown in Fig. 1-a. The micropipette is loaded with solution when dipped into a solution reservoir due to the capillary force. The solution is continuously released of the needle by vibration and deposited on the substrate with the micropipette moving along a predefined path during the printing process. Finally, we obtain a tunable morphology of crystal films of organic and perovskite semiconductors, including remarkably aligned crystals with high electrical performance. Furthermore, we produce active photodetector arrays based on OTFT and a perovskite with the large-area, low-temperature direct-write printing technology.

2. Results and discussion

Crystal morphology

The speed of printing makes a great influence in crystal morphology both in TIPS-pentacene and perovskite. (Fig. 1-b). By varying the moving speeds as 100 μm/s, 400 μm/s, and 1000 μm/s when depositing solution of TIPS-pentacene, three different morphologies are obtained including small pieces of plate-like crystals, thin crystalline belts along the printing direction, and isotropic, spherical crystals. (upper) When depositing the perovskite MAPbI₃ solution (10 wt%) at speeds of 50 μm/s, 100 μm/s, and 500 μm/s, a change of morphology was also observed. The morphology changes from very uniformly aligned, crystalline belts along the printing direction to randomly oriented crystalline belts. (below)

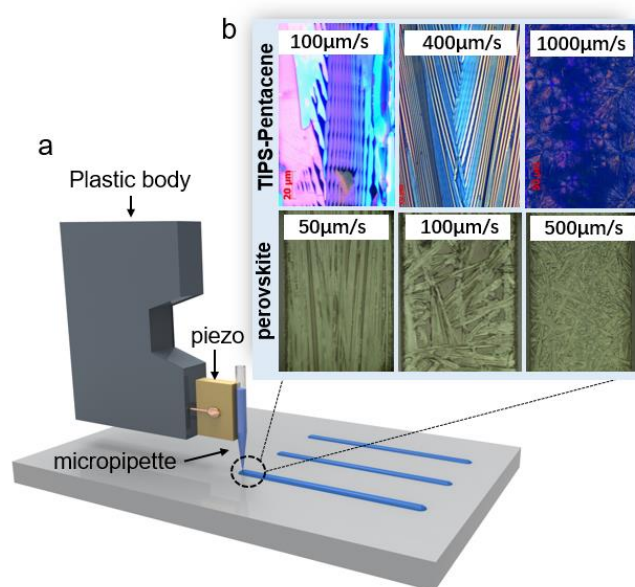


Fig. 1 a. A schematic representation of the ultra-sonic vibrated dispenser. b. Polarized optical microscope (POM) images of TIPS-pentacene and perovskite crystals printed at different speeds.

Organic transistor

The OTFTs based on TIPS-pentacene in the bottom-gate, top-contact configuration with SiO₂ as the gate insulator and Au as the source/drain electrodes are fabricated. The transfer characteristics of OTFTs based on TIPS-pentacene deposited at various speeds (100 to 1000 μm/s) are investigated (Table I). The optimized devices with aligned crystals (printed at 400 μm/s) exhibit the highest current and mobility value as compared with those with less ordered crystals

deposited at either a higher or lower speed (Fig 2-b).

Printing speed($\mu\text{m/s}$)	Mobility ($\text{cm}^2/\text{V}\cdot\text{S}$)	$I_{d(\text{ave})}$ (A)
100	0.19	$1.24 \cdot 10^{-5}$
200	0.24	$2.26 \cdot 10^{-5}$
400	0.47	$5.68 \cdot 10^{-5}$
800	0.15	$2.18 \cdot 10^{-5}$
1000	0.03	$3.08 \cdot 10^{-6}$

Photodetector

The perovskite-based photodetectors are fabricated with vacuum-deposited gold source and drain on the top of the perovskite MAPbI_3 film deposited under ambient conditions. The devices are characterized under ambient conditions, and channel current is measured under illumination (white light) and in the dark. The photocurrent of perovskite MAPbI_3 photoconductors printed at different speeds are measured. It is worth to note that the films printed at speeds under $100 \mu\text{m/s}$ exhibit an apparent photocurrent of nearly 100 times higher than the film printed at $500 \mu\text{m/s}$ when biased at -15 V . The photo to dark current ratio ($I_{\text{ph}}/I_{\text{dark}}$) is presented in Fig. 2-a, which shows that the photocurrent of films printed at $100 \mu\text{m/s}$ increases linearly with drain voltage.

Active photodetector.

As shown above, the OTFTs exhibit a strong gate-tuning effect, while the photodetectors exhibit a clear photo-response. Notice that the OTFTs exhibit a negligible photo-response, and the perovskite photodetectors do not show gate-tunability with a constant current in air. However, the active-matrix of a photo-detector calls for a stable off-state at zero gate-bias to maintain low power consumption. Therefore, we combine the advantages of the two devices to make gate-tunable, or electrical-switchable photodetectors. The characteristics of an individual photo-detecting cell is shown in Fig.2-c, where a perovskite photodetector is connected to the drain electrode of a TIPS-pentacene OTFT. The device is scanned by sweeping the gate voltage and setting the source-drain voltage as $V_d = -1 \text{ V}$. Without gate biasing, the detecting cell is not conductive even with illumination because of the low conductivity of the OTFT. At gate voltages larger than the threshold and with illumination, the conductivity of the both OTFT and photodetector sharply increase. The transient response of the detector cell is measured by periodic illumination (Fig.2-d) and shows a stable response to light switching. Because of the small W/L and ambient fabrication conditions, the light to dark current ratio is limited to approximately 100, which can be further enhanced by optimizing the fabrication and using a larger W/L ratio.

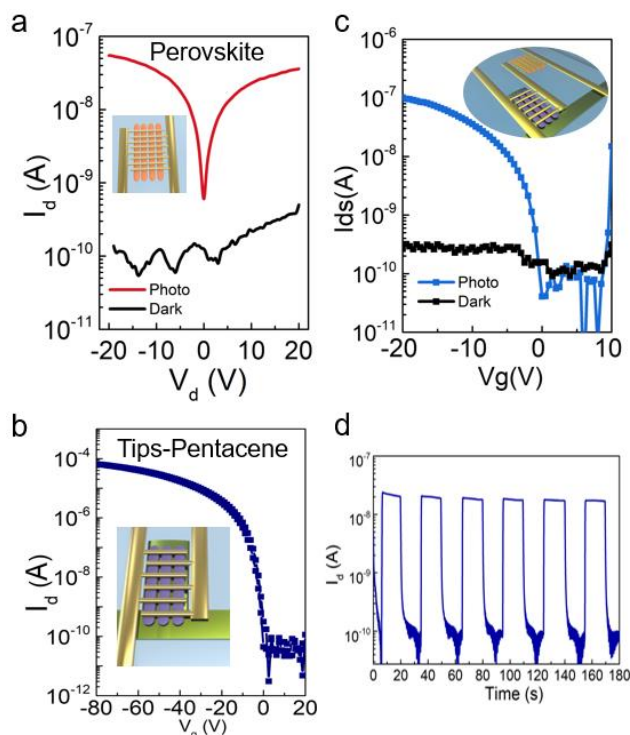


Fig. 2 a. Photo-electric response currents of photodetectors using MAPbI_3 . b. Transfer characteristic curves of the OTFT based on Tips-pentacene. c. OTFT-photodetector cell measured under light or dark conditions (at $V_d = -1 \text{ V}$) d. The transient response of an OTFT-photodetector cell with periodic illumination.

3. Conclusions

The guided crystallization of organic and perovskite semiconductors has been achieved by printing solutions with the ultra-sonicated dispenser. From slow to high moving speeds, the dispenser generates plate-like crystals, aligned crystalline belts, and spherical crystals. Highly ordered, aligned TIPS-pentacene and perovskite MAPbI_3 semiconductors have been obtained using an optimized moving speed of the dispenser. The TFT and photodetector devices utilizing aligned crystals exhibit higher on-currents than those devices with disordered crystals. Finally, we combine the two types of devices and demonstrate an OTFT-controlled photodetector for visible-light-sensing. The detector cell switches from the off-state to the on-state only with both illumination and gate-tuning and works well under ambient conditions. The presented studies demonstrate the potential of using the ultra-sonicated dispenser to print electronic and opto-electronic devices.

References

- [1] Deng, W.; Zhang, X.; Huang, L.; Xu, X.; Wang, L.; Wang, J.; Shang, Q.; Lee, S.-T.; Jie, J. *Advanced Materials* 2016, 28, 2201-2208
- [2] Giri, G.; Park, S.; Vosgueritchian, M.; Shulaker, M. M.; Bao, Z. *Advanced materials* 2014, 26 (3), 487-493
- [3] James, D. T.; Frost, J. M.; Wade, J.; Nelson, J.; Kim, J. S. *Acs Nano* 2013, 7 (9), 7983-7991.
- [4] Gu, X.; Shaw, L.; Gu, K.; Toney, M. F.; Bao, Z. *Nature communications* 2018, 9 (1), 534.